remote sensing

MDPI

Article

Performance Assessment of Global-EO-Based Precipitation Products against Gridded Rainfall from the Indian Meteorological Department

Nitesh Awasthi [1], Jayant Nath Tripathi [1], George P. Petropoulos [2], Dileep Kumar Gupta [3,*], Abhay Kumar Singh [3] and Amar Kumar Kathwas [4]

[1] Department of Earth & Planetary Sciences, University of Allahabad, Prayagraj 211002, Uttar Pradesh, India; niteshawasthi88@gmail.com (N.A.); jntripathi@gmail.com (J.N.T.)
[2] Department of Geography, Harokopio University of Athens, El. Venizelou St., 70, Kallithea, 17671 Athens, Greece; gpetropoulos@hua.gr
[3] Department of Physics, Institute of Science, Banaras Hindu University, Varanasi 221005, Uttar Pradesh, India; singhak@bhu.ac.in
[4] Haryana Space Applications Centre, Hisar 125004, Haryana, India; kathwas.amarkumar@gmail.com
* Correspondence: dileepgupta85@gmail.com

Abstract: Monitoring water resources globally is crucial for forecasting future geo-hydro disasters across the Earth. In the present study, an attempt was made to assess the functional dimensionality of multi-satellite precipitation products, retrieved from CHIRPS, NASA POWER, ERA-5, and PERSIANN-CDR with respect to the gridded India Meteorological Department (IMD) precipitation dataset over a period of 30+ years (1990–2021) on monthly and yearly time scales at regional, sub regional, and pixel levels. The study findings showed that the performance of the PERSIANN-CDR dataset was significantly better in Central India, Northeast India, and Northwest India, whereas the NASA-POWER precipitation product performed better in Central India and South Peninsular of India. The other two precipitation products (CHIRPS and ERA-5) showed the intermediate performance over various sub regions of India. The CHIRPS and NASA POWER precipitation products underperformed from the mean value (3.05 mm/day) of the IMD gridded precipitation product, while the other two products ERA-5 and PERSIANN-CDR are over performed across all India. In addition, PERSIANN-CDR performed better in Central India, Northeast India, Northwest India, and the South Peninsula, when the yearly mean rainfall was between 0 and 7 mm/day, while ERA-5 performed better in Central India and the South Peninsula region for a yearly mean rainfall above 0–7 mm/day. Moreover, a peculiar observation was made from the investigation that the respective datasets were able to characterize the precipitation amount during the monsoon in Western Ghats. However, those products needed a regular calibration with the gauge-based datasets in order to improve the future applications and predictions of upcoming hydro-disasters for longer time periods with the very dense rain gauge data. The present study findings are expected to offer a valuable contribution toward assisting in the selection of an appropriate and significant datasets for various studies at regional and zonal scales.

Keywords: rainfall; IMD; CHIRPS; NASA POWER; ERA-5; PERSIANN-CDR

check for updates

Citation: Awasthi, N.; Tripathi, J.N.; Petropoulos, G.P.; Gupta, D.K.; Singh, A.K.; Kathwas, A.K. Performance Assessment of Global-EO-Based Precipitation Products against Gridded Rainfall from the Indian Meteorological Department. *Remote Sens.* **2023**, *15*, 3443. https://doi.org/10.3390/rs15133443

Academic Editors: Guido D'Urso and Yuanjian Yang

Received: 5 April 2023
Revised: 5 June 2023
Accepted: 29 June 2023
Published: 7 July 2023

Copyright: © 2023 by the authors. Licensee MDPI, Basel, Switzerland. This article is an open access article distributed under the terms and conditions of the Creative Commons Attribution (CC BY) license (https://creativecommons.org/licenses/by/4.0/).

1. Introduction

The water cycle is an essential physical process for life on Earth. In atmospheric events studies, precipitation in the form of rainfall tends to be one of the most important parameters to be studied in broad ways [1]. Water enters the terrestrial surface largely through precipitation and influences the dynamics of the environment. A consistent long-term record of a fine spatiotemporal resolution of global precipitation is very important for various applications such as irrigation scheduling, crop yield forecasting, water resource management, hydrometeorology, flood and drought monitoring, and hydrological modeling applications. The Indian monsoon plays an important role in the Earth's climate and the water cycle as a key part of the South-Asian monsoon where the deep convection force plays a crucial role [2,3]. The southwest monsoon influences different components of Indian livelihoods such as agriculture, industry, the energy sector, and the domestic household. India receives a substantial amount of precipitation during the period of June–August due to the southwest monsoon and during November–January owing to the Northeast monsoon annually, relating to the temporal variability in the topography accordingly [3–5]. Climate change has affected the Indian monsoon system significantly, which has influenced the annual recharge of water sources in the country [2,6]. In recent years, the areas located in the parts of Himalayan region have faced drastic flood events and cloud bursts due to high-intensity precipitation.

Ground-based rain gauge measurements of precipitation provide an accurate measurement at the point locations with inadequate spatial resolution and their heterogeneous distribution [1]. However, information of precipitation variability at large scales requires a reliable model or a reanalyzed dataset of the hydro-geological cycle at the finest spatiotemporal resolution covering various topographic terrains and oceans [7]. Nevertheless, their efficiency and accuracy can be improved by their regular evaluation concerning ground-based measurements, which will enhance the modeling capability including validation and calibration processes. Researchers performed an investigation to assess 120 years of rainfall dynamics in the Haryana state of India using the statistical variables of mean rainfall, rainfall deviation, moving-average, rainfall categorization, rainfall trend, correlation analysis, and the probability distribution function. The outcome of the study revealed that rainfall in almost all parts of the state is declining [8]. In the cases of India and its adjoining regions, infrared-sensor-based precipitation monitoring algorithms were developed by the Indian Space Research Organization (ISRO) in 2002, after the successful launch of Kalpana-1, which provides precipitation estimations with remarkable resolution and accuracy [9]. A validation of INSAT-3 D rain estimates and the Global Land Data Assimilation System (GLDAS) with IMD rainfall products was carried out. The observed correlation of 0.83 showed a significant amount of acceptability [10]. The data obtained from the Kalpana-1 Satellite are greatly utilized for the monitoring of precipitation patterns and intensity along with the occurrence of drought events during the monsoon season in India [10–13]. The infrared-sensor-based precipitation algorithms are also combined with the INSAT-3D satellite observations to achieve an even finer spatial resolution in comparison to the Kalpana-1 estimates. However, in infrared-satellite-based precipitation products, rainfall is underestimated across orographic precipitations due to the orographic air lift in mountain terrain across the country.

The infrared- and microwave-sensor-based precipitation measurements enable the estimation of precipitation at significant spatial and temporal variabilities, globally. The precipitation estimation improved substantially after the launch of the Tropical Rainfall Measuring Mission (TRMM) satellite, which provided precipitation datasets at relatively high temporal and spatial resolution since November 1997 [14–16]. The real-time TRMM-recorded meteorological parameters are widely used around the world for planning and prediction of the different atmospheric phenomena on different terrains [17,18]. Researchers have developed an algorithm named Integrated Multi-Satellite Retrievals for GPM (IMERG), which integrates the data obtained from all the GPM satellite constellations for the estimation of precipitation, demonstrating better performance compared to TRMM over India [17,19–21]. However, the limited temporal availability of the IMERG and TRMM-based multi-satellite precipitation products has been inadequate in many climatological applications since 2014 and 1998, respectively. Therefore, several precipitation products have been developed to bridge the data accessibility with high temporal (hourly or daily) and spatial resolution prior to the year of 1990. The ERA5 fifth-generation reanalysis data are produced by the Copernicus Climate Change Service (C3S) of ECMWF, which are available on an hourly scale from 1950 onward with a spatial resolution of 0.28° [22];

moreover, the Climate Hazards Group InfraRed Precipitation with Station data (CHIRPS) dataset on a daily scale is available from 1981 to the present [23]. The other precipitation datasets, viz., the Precipitation Estimation from Remotely Sensed Information using Artificial Neural Networks-Climate Data Record (PERSIAN-CDR) and NASA POWER products, are also available from 1983 and 1981, respectively. A validation was conducted on daily and monthly satellite-based rainfall data from the Climate Hazards Group InfraRed Precipitation with Station data (CHIRPS), Global Precipitation Measurement (GPM), and PERSIANN using the publicly available rainfall field data from 1990 to 2020 [24]. The study findings showed that the CHIRPS data outperformed the other datasets with a ratio closer to one. The comparison of the monthly rainfall datasets from GPM, Climatic Research Unit (CRU), CHIRPS, GLDAS, PERSIANN-CDR, SM2RAIN, and TerraClimate with IMD gridded rainfall data was also assessed in the same study [25]. The authors demonstrated that the GPM dataset typically ranks as a good-performing fit, followed by CHIRPS and then PERSIANN-CDR; however, despite its finer resolution, the TerraClimate dataset performs poorer at the pixel level [25].

Even though IMERG and TRMM-era precipitation products perform better in India, these products were not taken into consideration in the present investigation, due to the limitation related to the temporal availability of datasets. Despite the fact that there are not many research studies available to assess how accurate the precipitation is in India for the time span of 30 or more years, the CHIRPS, NASA POWER, ERA 5, and PERSIANN CDR rainfall datasets are used for the present analysis because of their long-term availability of more than 30 years. Currently, the performance of CHIRPS and PERSIAN-CDR datasets has been evaluated against IMD-rain-gauge-based observations by researchers over India for the time period of 10–15 years only. However, the performance of the NASA POWER precipitation product has not been or very seldom been evaluated [14,20]. In addition, the reanalysis precipitation datasets, namely, PERSIAN-CDR, CHIRPS, and ERA5, also utilize the cloud-based computing facility on Google Earth Engine (GEE) which is a cloud-based computational platform that provides access to numerous geospatial datasets [26–28].

In purview of the above, the primary objective of the present investigation is to assess the performance of CHIRPS, ERA5, PERSIAN-CDR, and NASA POWER precipitation products against IMD gridded datasets in monthly and yearly time spans at regional, sub regional, and pixel scales for the long term (30+ years) over India. This is important, as the study findings may provide more confidence in selecting rainfall products for various applications. The comparative performance and the recommendation for the better-performing dataset on different time scales at regional, sub regional, and pixel scales for the long term are also reported among these datasets. This study will facilitates the selection of the best-performing rainfall dataset for various applications and offers more details regarding a region's rainfall pattern. This means that it also offers helpful advice to agricultural stakeholders when they are making operational choices.

2. Datasets and Methodology

2.1. Study Area

The precipitation-observing technologies have various challenges regarding reasonably representing the climate of a region because India is widely enriched with natural resources with its complex topography. Cultural diversity based on terrestrial resources has spread throughout the subcontinent of India including neighboring countries, which are politically apart from India.

Furthermore, India is divided into four sub regions to compare the precipitation products in different parts of India according to the IMD region-wise rainfall maps (https://mausam.imd.gov.in/responsive/rainfallinformation_msd.php accessed on 20 January 2023). The northwest sub region contains higher Himalayan, lower Himalayan, and plane terrestrial regions of India [29]. The major rivers of Himalayan origin are flowing in these sub regions, which makes these lands most fertile for numerous crops that have socioeconomic importance in India [30,31]. The central Indian region comprises the Satpura-

Aravali Gondwana basin from east to west, which is located over the Pachmarhi plateau and part of the Central Indian Techtronic Zone (CITZ) in India [32]. The Northeast sub region represents the easternmost part of India, which is united by seven hilly forest states of India. The northeast terrestrial regions encompass a subtropical climate that is influenced by the southwest monsoon along with the Meghalaya Plateau, which is known to be a heavy precipitation-receiving area in India [4,33]. The hydro-winds originating from the Bay of Bengal circulates the maximum amount of annual precipitation in these parts. The Southern Peninsula is also called the Indian shield due to its stable geological characteristic on account of the ancient rocks, liable surface, and river-dominant land. It was formed after the separation of the Gondwanaland rift along the eastern and western margin, stabilizing during a long time period across major Himalayan terrain from Antarctica-Australia around the early Cretaceous period (130 My). The historic geogenic uplift and reactivation of faults are primarily associated with the Himalayan Orogeny and the whittling of the topography of these lands [34]. Figure 1 depicts the study area along with the locations of IMD scattered rain gauge stations (2868 stations during August 2022), i.e., India as a whole and its various regions (Northwest, Northeast, Central, and South Peninsula) where the present study was carried out.

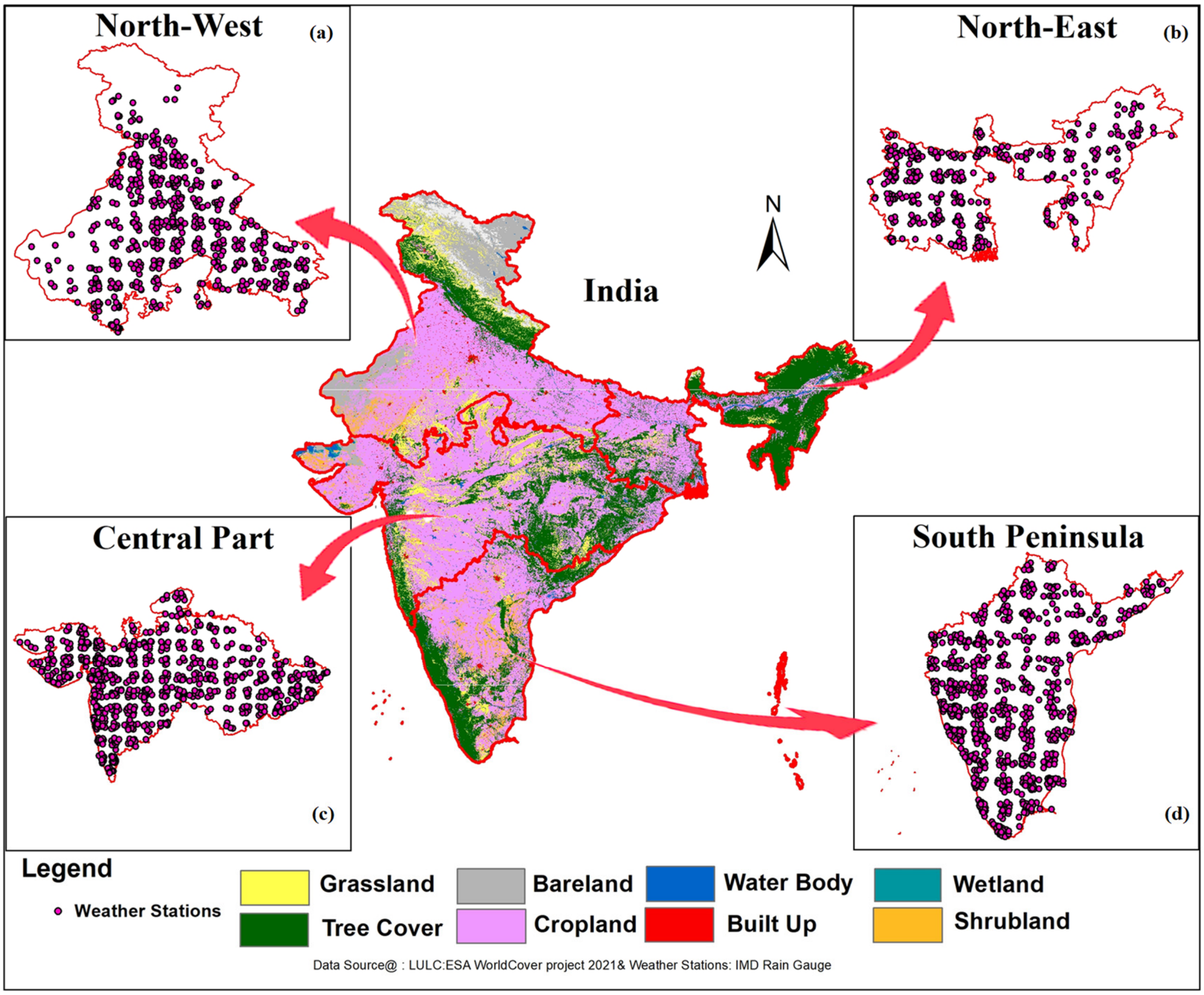

Figure 1. India and sub regions of India, namely, (**a**) Northwest India, (**b**) Northeast, (**c**) Central India, and (**d**) South Peninsula with IMD rain gauge locations over India during August 2022.

These rain gauges provided diurnal observations during the month of August. The total number of 2868 rain gauges are available on August 2022.

2.2. Precipitation Datasets

Table 1 shows descriptions of the all-precipitation data products used in the current investigation. The gridded-precipitation daily data product developed by IMD with a well-spread rain gauge network (total of 6955 rain gauge stations with varying availability during the period of 1901–2010 in India at present established by either state governments, agricultural universities, and the central government body, namely, IMD [35]) across the country provides datasets in the grid format from the year 1901 for significant climatological applications; however, a lack of rain gauge stations can be observed in the northern and northeast regions. On the contrary, the Global Precipitation Climatology Centre (GPCC) records precipitation data from approximately 400 gauge stations scattered around India [36]. The combination of several stations across India makes IMD more powerful and effective than GPCC. Figure 1 provides the PAN India density of 2868 rain gauge stations installed by IMD only during August 2022.

Table 1. Description of the precipitation data products (sources with their spatial and temporal resolution).

Datasets Name and Sources	Spatial Resolution	Temporal Resolution	Data Availability
IMD Gridded Data (https://www.imdpune.gov.in/lrfindex.php, accessed on 3 January 2023)	0.25°	Daily	1901–Present
CHIRPS (https://data.chc.ucsb.edu/products/CHIRPS-2.0/, accessed on 6 January 2023)	0.05°	Daily	1981–Present
NASA POWER (https://power.larc.nasa.gov/beta/data-access-viewer/, accessed on 9 January 2023)	0.5°	Daily	1981–Present
ERA5 (https://cds.climate.copernicus.eu/cdsapp#!/home, accessed on 14 January 2023)	0.1°	Daily	1950–Present
PERSIANN-CDR (https://chrsdata.eng.uci.edu/, accessed on 18 January 2023)	0.25°	Daily	1983–Present

The various satellite-based or reanalysis precipitation products, namely, CHIRPS, ERA5, PERSIANN-CDR, and NASA POWER, along with IMD gridded precipitation datasets for the period of 1990–2021, were downloaded from respective data providing agency portals. The gridded data combine ground-based gauge observation as well as infrared satellite cold cloud duration measurements. The latest versions of the datasets were used in this study.

The United States Geological Survey (USGS) in collaboration with Climate Hazard Group (CHG) developed a CHIRPS precipitation data product at a global (50°S–50°N) scale for the monitoring of seasonal precipitation dynamics and droughts. This dataset is available for various time scales such as daily, pentad, dekad, monthly, 2-monthly, 3-monthly, and annual time scales and ranging from 1981 to near-present.

ERA5 is a recent and fifth-generation global climate ECMWF atmosphere reanalysis dataset. It is the descendant of ERA-Interim datasets, which was released in 2006. ERA5 datasets are produced using the four-dimensional variation data assimilation utilizing the numerical model known as the ECMWF Integrated Forecasting System (IFS) for collecting data from distinct observational systems (ground-based, atmospheric boundaries, and satellite radiance) into a comprehensive analysis of atmospheric parameters. The datasets are provided in gridded format with a spatial resolution of 9 km [22].

The PERSIANN-CDR precipitation dataset is based on infrared temperature imaging. The algorithm is generated through geostationary satellite observations. The precipitation estimation is achieved from infrared information using an Artificial Neural Network

(ANN) algorithm. The recorded information is calibrated using the adaptive training algorithm on the microwave data and updates the network parameters of the microwave precipitation estimation [1]. The PERSIANN-CDR diurnal precipitation estimates with a 0.04° spatial resolution at a 3-hourly temporal interval for the period ranging from 1983 to the present are available since 1981. The Gridded dataset is available in the public domain by the product name GridSat-BI with infrared as its main input. The monthly Global Precipitation Climatology Project (GPCP) version 2.2 product is used for the calibration of the PERSIANN-CDR datasets [37].

The NASA POWER project provides an open data source of meteorological parameters as a gridded gauge-product of the Global Precipitation Climate Project (GPCP v2.1), which is attributed to a spatial microwave imager with a resolution of 0.5°, providing a fractional occurrence of precipitation over the target terrain [38]. This algorithm uses geostationary IR, a low-orbit IR, and atmospheric-infrared-sounder-sensor-based observations. The NASA POWER dataset is empowered with a 0.1° spatial resolution and diurnal temporal time-series in UTC time, and covers a 15° swath of longitude at local solar time (LST).

2.3. Methodology

The performance evaluation of respective precipitation products was carried out on monthly and yearly time scales with a spatial resolution of 0.25° (rain-gauge-based IMD product) for the period of 1990–2021, since IMD provides the gauged precipitation dataset at a spatial scale of 0.25°.

The performance evaluation of various precipitation products in comparison with the IMD rain gauge gridded precipitation product was carried out using various performance indices for spatial and temporal distributional patterns at regional, sub regional, and pixel levels on monthly and yearly time scales. All the precipitation products were resampled similar to the reference datasets (IMD gridded dataset) due to the spatial and temporal heterogeneity. In order to perform a comparative assessment between IMD and satellite-derived precipitation datasets, the aggregation of datasets is necessary since IMD collects daily precipitation at 0300UTC, which is distinct from the daily satellite precipitation accumulation convention [36]. Therefore, monthly and yearly mean precipitation was computed for various satellite-based precipitation products. Furthermore, to obtain the spatial equality in order to perform a comparative investigation, all the datasets were resampled to a pixel size of 25 km using the nearest-neighbor resampling technique. Since the present investigation is pixel-based, assessment of the performance of the datasets was performed at each pixel-scale area.

The continuous statistical parameters were calculated for the estimation of bias, mean, coefficient of variance (CV), root-mean-square error ($RMSE$), and Pearson's correlation coefficient (r) for each grid/pixel across India for the target period using the yearly datasets. Furthermore, random and systematic errors for the datasets were also estimated using decomposition techniques. The estimation of parameters was performed using the following relations [36]:

$$r = \frac{\sum_{i=1}^{n}(G_i - G)(S_i - S)}{\sqrt{\sum_{i=1}^{n}(G_i - G)^2 \sum_{i=1}^{n}(S_i - S)^2}} \tag{1}$$

$$Bias = S - O \tag{2}$$

$$CV = \frac{\sqrt{\frac{\sum_{i=1}^{n}(S_i - S)^2}{n}}}{S} \times 100\% \tag{3}$$

$$RMSE = \sqrt{\frac{\sum_{i=1}^{n}(S_i - G_i)^2}{n}} \tag{4}$$

$$System\ Error = \frac{\sum_{i=1}^{n} (S_i{}^* - G_i)^2}{n} \tag{5}$$

$$S_i{}^* = a \times G_i + b \tag{6}$$

where S_i represents the satellite-attained precipitation and G_i denotes the gauge-based precipitation, with S and G being their respective mean; n is the total number of observations; and a and b represent the gradient and intercepts, respectively. The ideal value of error and r is 0 and 1, respectively.

In addition, another very important performance index, namely, the modified Kling–Gupta efficiency score (KGE), was computed to assess the performance of satellite-derived precipitation datasets against gauged precipitation data. This performance index provides the performance result in combination with the three performance indices, viz., Pearson's correlation coefficient, bias, and variability [6,38].

Model performance criteria are often used during the calibration and evaluation of models to express in a single number the similarity between observed and simulated values. Traditionally, the Nash–Sutcliffe Efficiency (NSE) is an often-used metric as it normalizes model performance into an interpretable scale. The Kling–Gupta Efficiency (KGE) addresses several shortcomings in NSE and is increasingly used for model calibration and evaluation [39]. Like NSE, a KGE value of 1 indicates perfect agreement between simulated and observed values. The KGE score was computed using the equation given below.

$$KGE = 1 - \sqrt{(r-1)^2 + (\beta - 1)^2 + (\gamma - 1)^2} \tag{7}$$

where β and γ represent the bias variability ratio. The optimum values of KGE, β, and γ are 1.

3. Results and Discussion

3.1. Temporal Trend of Precipitation Products over India and Its Sub Regions

The temporal time series of the monthly average precipitation product is also obtained over India and four sub regions of India, viz., Central India, Northeast, Northwest, and South Peninsula regions, derived from IMD, CHIRPS, NASA POWER, ERA-5, and PERSIANN-CDR for 30+ years (1990 to 2021) (Figure 2a–e). It is observed that all the products show a similar trend with distinct errors, except in the northeast of India. However, IMD-gauge-based precipitation data showed elevated peaks rather than multi-satellite-based products. Northeast India receives comparatively higher rainfall than other parts of India. The gauge-based product triumphs in capturing precipitation datasets in such areas where satellites are deficient in observing actual data points because of highly dense clouds in these parts [40]. High terrestrial altitudes of Himalayan foothills also influence the capture of precipitation using satellite sensors. A similar temporal trend is detected in the central and northwest regions. However, the northwest region receives comparatively lower precipitation than central India. A persisting temporal variability in precipitation is observed in the South Peninsula. In regards to this point, a recent study demonstrated an upcoming precipitation extreme in the Southern Peninsula that is indicated by the previous temporal trend of precipitation [30].

Climate change invokes alterations in the regional hydrological cycle and the surface temperature plays a crucial role in such phenomena. Extreme temperature accelerates the hydro-evaporation led by the high atmospheric transport of water vapor, quantitatively. A long-duration high dip is observed in India during the years 1994–2010. The temporal trend of precipitation in India during the study period shows an average rainfall that spiked in 2003 following the average local extreme in the country, which is also shown in a similar study [36].

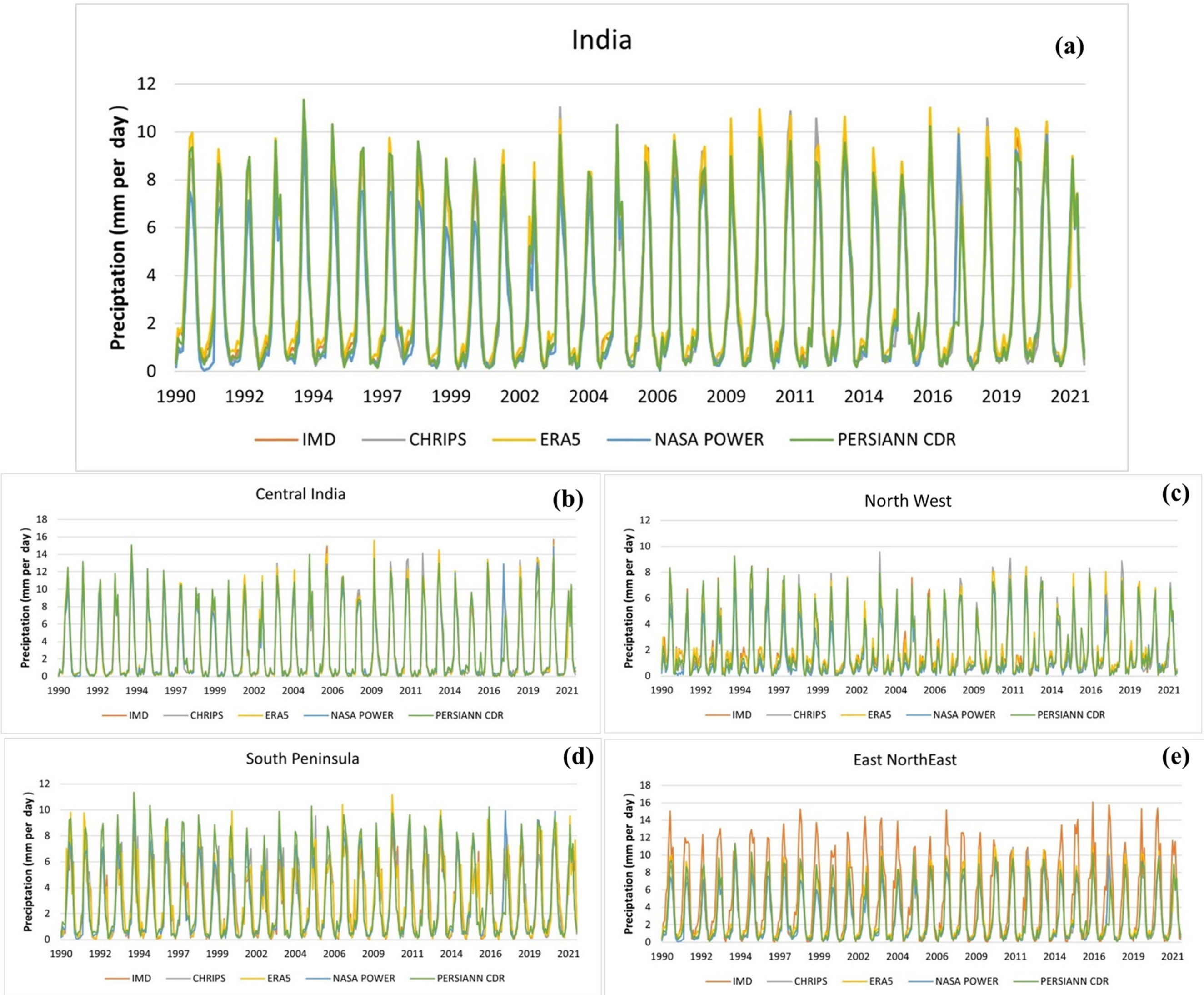

Figure 2. The temporal trend of monthly average precipitation over India obtained from IMD, CHIRPS, NASA POWER, ERA-5, and PERSIANN-CDR from the years 1990 to 2021 (**a**) over India, (**b**) Central India, (**c**) Northwest, (**d**) South Peninsula, and (**e**) East Northeast.

In order to assess the temporal trend and magnitude of variation in the values of the precipitation products compared to IMD's rain gauge station values, a scatter plot is created between the average monthly and yearly precipitation values of IMDs and the values obtained from respective precipitation products (Figure 3a,b). Figure 3a,b show the scatterplot between the monthly and yearly averaged IMD gridded precipitation dataset and other multi-satellite products (CHIRPS, NASA POWER, ERA-5, PERSIANN-CDR) over India and its sub regions (Northwest India, Northeast India, Central India, and South Peninsula), respectively, with performance indices like the Pearson correlation and RMSE value. The performance of multi-satellite products is found to be better for monthly time scales over India and its sub regions than for yearly time scales. The values of the correlation coefficient and RMSE are found to be 0.99–0.95 and 0.42–1.25 mm/day for all the multi-satellite precipitation products over all India and its sub regions, respectively. The highest value of RMSE is found for PERSIANN-CDR over the Northeast region, which is an indication of the comparatively lower performance of PERSIANN-CDR in this region than other products and regions on monthly time scales. The lowest value of RMSE is found to be 0.42 mm/day over the Northwest part of India for the NASA POWER precipitation product, showing its better performance than other products and regions on monthly time scales. The other precipitation products and regions on monthly time scales show intermediate performance. The values of the correlation coefficient and RMSE are found to be 0.93–0.36 and 0.16–1.48 mm/day for all the multi-satellite precipitation products over all India and its sub regions for yearly time snaps, respectively. The lowest RMSE is found to be 0.16 mm/day for ERA-5 for Central India, showing a better performance than other products on yearly time scales. However, the highest value of the RMSE is found to be 1.48 mm/day for the regions Northeast and ERA-5, showing the lowest performance on yearly time scales. High variations in performance indices are found for various multi-satellite precipitation products over all India and its sub regions on yearly time scales than monthly time scales. However, a higher performance is found for all the various multi-satellite precipitation products over India and its sub regions on monthly time scales than yearly time scales. The lowest performance of all multi-satellite precipitation products is found for the Northeast region on monthly and yearly time scales.

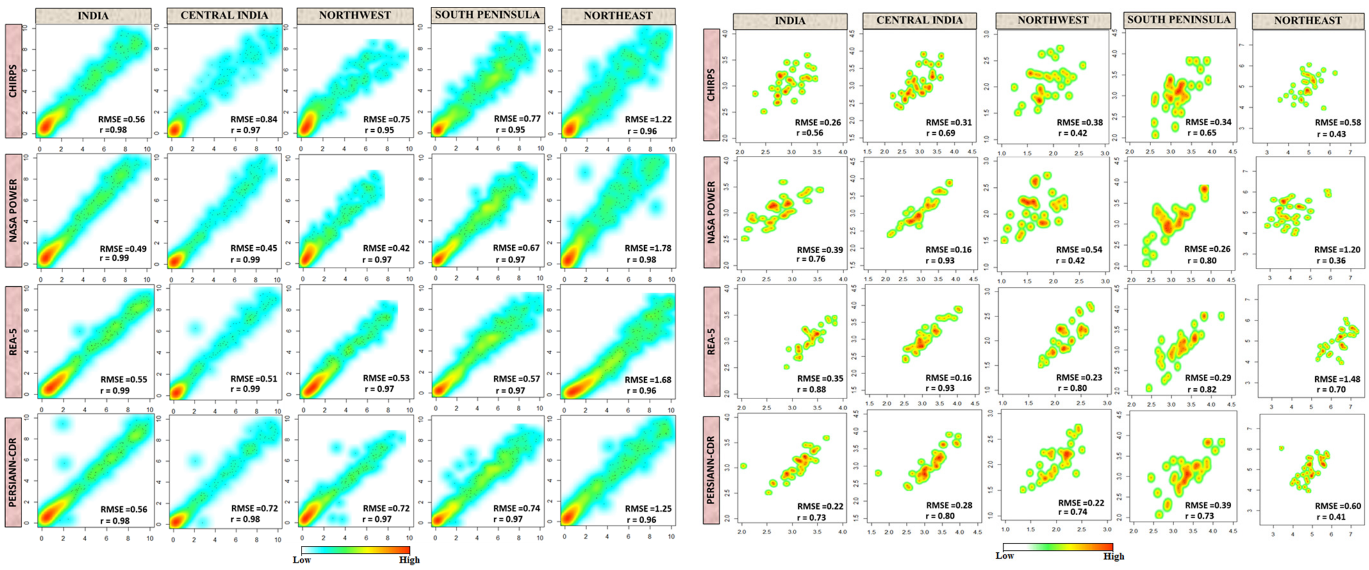

(**a**) (**b**)

Figure 3. Scatterplot of average rainfall data on (**a**) monthly scale and (**b**) yearly scale over India and its sub regions (Northwest India, Northeast, Central India, and South Peninsula) between IMD and (CHIRPS, NASA POWER, ERA-5, PERSIANN-CDR) during the years from 1990 to 2021. The color bar represents the density of data points.

From Figure 4, it can be observed that the high-precipitation areas are observed in the west and north coast, northeast and central India by the multi-satellite products, which is a well-known fact already. However, each product gives notably slightly different magnitudes over the same region. A precipitation gradient is formed along the west coast in IMD, ERA5, and CHIRPS products throughout the availability at higher native spatial resolution. Nevertheless, IMD captures the precipitation gradient in the northeast part of India, providing clearer imagery than the other four products. Due to the high density of gauge stations, IMD completes the information of rainfall at a finer level. However, the gauge-based precipitation dataset has a large uncertainty over the northern part of India, which is due to the lower density of rain gauge availability in these parts [35]. The rain gauge density is important for collecting rainfall information effectively and efficiently [41].

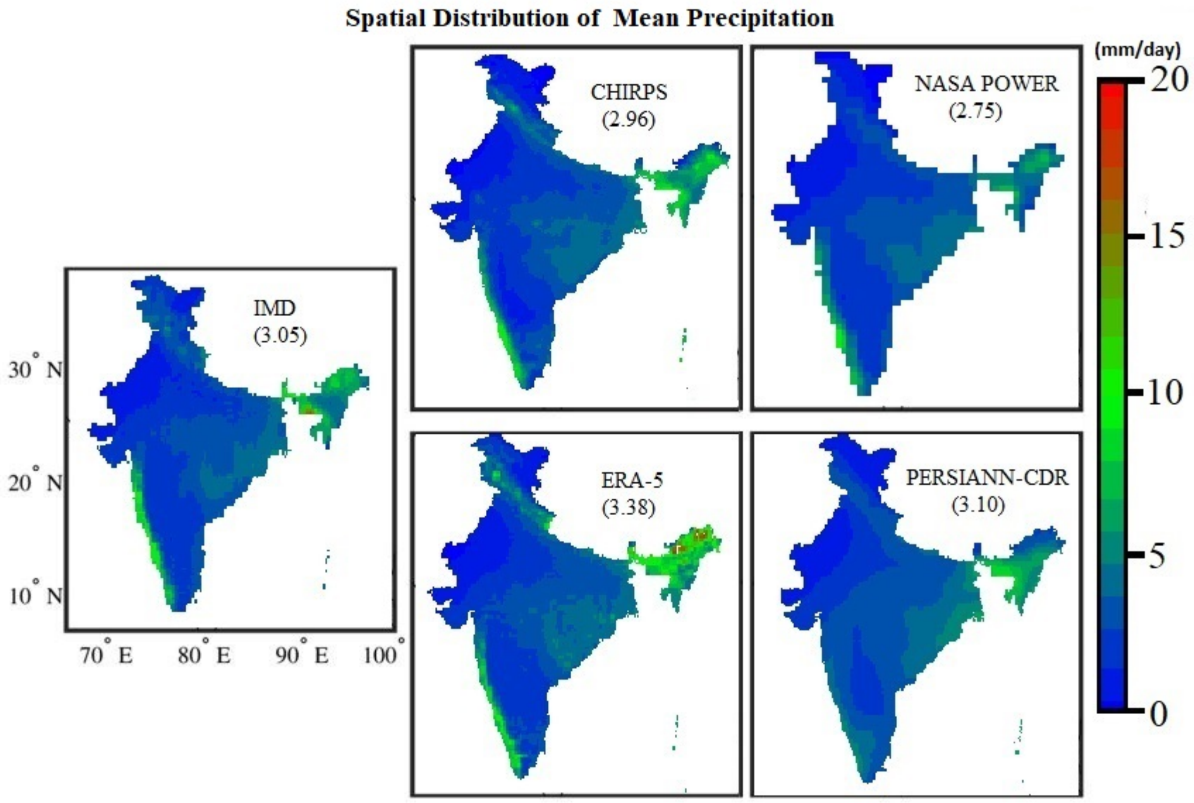

Figure 4. Spatial distribution of 32 years (1990–2021) of average precipitation (mm/day) across India from IMD, CHIRPS, ERA5, PERSIANN-CDR, and NASA POWER. The name of all datasets is reported along with each subplot.

3.2. Satellite-Derived Precipitation Products Performance over India at Pixel-Scale

The assessment of precipitation products is carried out using the correlation coefficients, RMSE, systematic error, bias, variability ratio, and KGE score over India and its sub regions at the pixel level for yearly time scales. The mean values of performance parameters over India at the pixel level for precipitation products are given in Table 2. All the satellite-based precipitation products, namely, PERSIANN-CDR, ERA-5, NASA POWER, and CHIRPS, show a significant correlation with the IMD-gauge-based precipitation over India at the pixel level for yearly time scales. The mean correlation coefficient (r) at the pixel level over India for yearly time scales is 0.54, 0.52, 0.47, and 0.44 for PERSIANN-CDR, ERA-5, NASA POWER, and CHIRPS, respectively. The highest value of correlation is found for PERSIANN-CDR, while the lowest correlation coefficient value is observed for CHIRPS. The ERA-5 and PERSIANN-CDR both attain a negative bias with values of bias of −0.33 mm/day and −0.05 mm/day, whereas CHIRPS and NASA POWER gain a positive bias with values of bias of 0.09 mm/day and 0.27 mm/day, respectively. A lower value of bias is found for PERSIANN-CDR, while a higher value of bias is observed for ERA-5. The RMSE mean values of 1.15 mm/day, 1.19 mm/day, 1.04 mm/day, and 1.07 mm/day are found for the PERSIANN-CDR, ERA-5, NASA POWER, and CHIRPS precipitation datasets at the pixel level over India for yearly time scales, respectively. The RMSE error is found to range from 1.19 to 1.04 mm/day, which is approximately the same for all the datasets. However, the systematic errors are found to be 4.93, 5.38, 3.76, and 4.63 percent for the PERSIANN-CDR, ERA-5, NASA POWER, and CHIRPS precipitation datasets, respectively. The lowest average RMSE and systematic error are found for the NASA POWER dataset, while the highest average RMSE and systematic error are found for the ERA-5 precipitation dataset and the intermediate values of average RMSE and systematic error are found for the PERSIANN-CDR and CHIRPS datasets over the Indian region at the pixel level for yearly time scales. Similarly, PERSIANN-CDR, ERA-5, NASA POWER, and CHIRPS are also assessed using mean values of modified KGE scores, which are obtained as 0.31, 0.28, 0.22, and 0.22, respectively. A higher value of mean modified KGE scores over the Indian region at the pixel level is found for the PERSIANN-CDR, while a lower value of mean modified KGE scores is observed for the NASA POWER and CHIRPS over India at the pixel level on yearly time scales. The mean values of modified KGE score over the Indian region at the pixel level suggests the usefulness of ERA-5 and PERSIANN-CDR for the modeling of precipitation data more efficiently over India.

Table 2. Computed mean values of the performance indices for the precipitation product of CHIRPS, NASA POWER, ERA-5, and PERSIANN-CDR against the IMD gauge-based precipitation data over India at the pixel level on yearly time scales.

	INDIA			
	CHIRPS	**NASA-POWER**	**ERA-5**	**PERSIANN-CDR**
Correlation coefficient	0.44	0.47	0.52	0.54
RMSE (mm day^{-1})	1.07	1.04	1.19	1.15
Systematic Error (%)	4.63	3.76	5.38	4.93
Bias	0.09	0.27	−0.33	−0.05
Variability Ratio	0.97	0.95	0.95	0.94
KGE	0.17	0.22	0.28	0.31

The four important performance indices (correlation coefficient, bias, variability ratio, and KGE) suggest that the PERSIANN-CDR data show better performance than the other precipitation datasets (ERA-5, NASA POWER, and CHIRPS). However, the other two performance indices (RMSE and systematic error) suggest intermediate performance for the PERSIANN-CDR datasets over India. The overall observation suggests the better performance of the PERSIANN-CDR datasets than the other precipitation datasets (ERA-5, NASA POWER, and CHIRPS).

Figure 5 illustrates the spatial distribution plot of the performance indices (correlation coefficients, bias, KGE score, RMSE, systematic error, and variability ratio) for the quantitative comparison of all four multi-satellite precipitation products (CHIRPS, NASA POWER, ERA-5, and PERSIANN-CDR) over the country as compared to the IMD gauge-based observations at the pixel level on yearly time scales for the target period of 1990–2021.

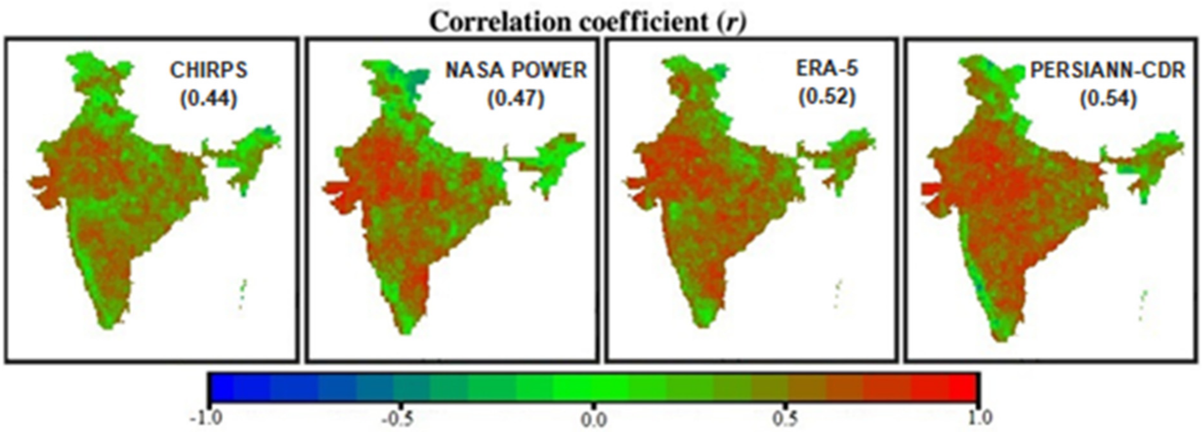

Figure 5. *Cont*.

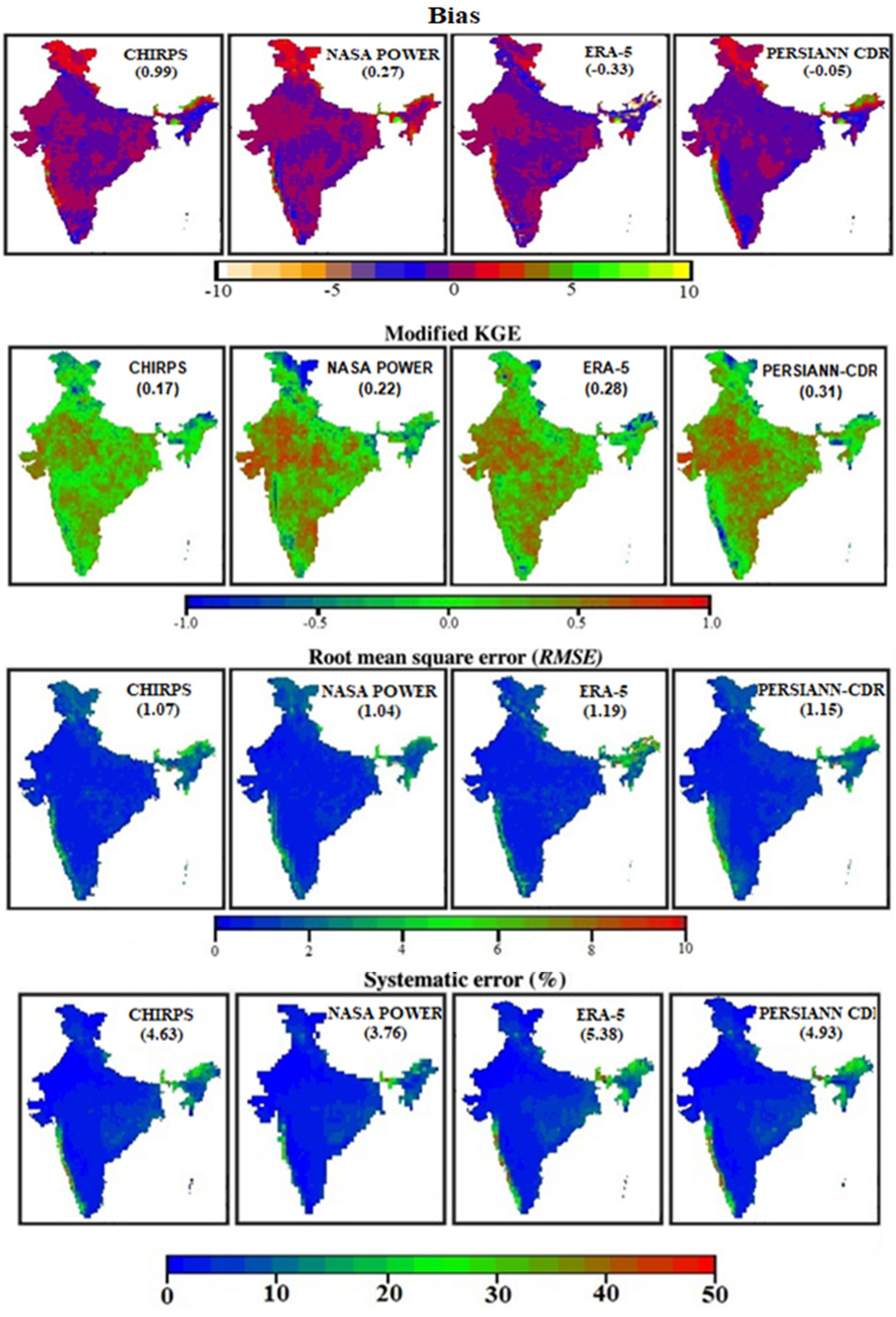

Figure 5. *Cont.*

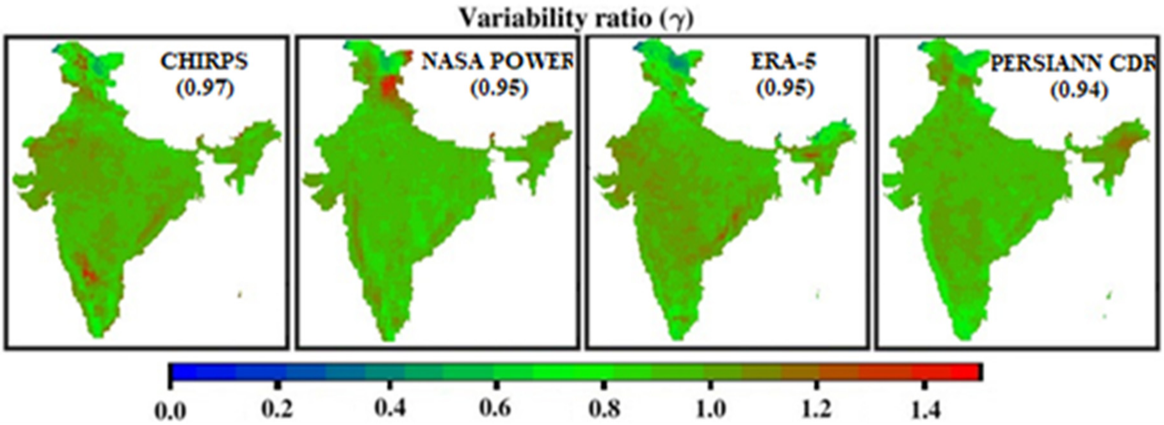

Figure 5. Spatial distribution of correlation coefficient (r), bias, modified KGE, RMSE, systematic error (percent), and variability ratio (γ) in yearly precipitation (mm/day) derived from CHIRPS, NASA POWER, ERA-5, and PERSIANN-CDR precipitation data for the period of 1990–2021 along with the IMD precipitation datasets over the country at the pixel level.

ERA-5 and PERSIANN-CDR show higher correlation coefficients concerning the IMD-gauge-based precipitation product. All four products show almost zero correlation in the Jammu–Kashmir–Ladakh region of North India, mainly because of the lack of ground-based gauges in these regions, indicating a larger uncertainty. The quantitative span of the estimation of correlation coincides with the mean precipitation over India is strongly depicted by ERA-5 and PERSIANN-CDR. In addition to that, ERA-5 shows a smooth distribution of the variability ratio over India and a gradient in the northeast region. The KGE score suggests that the PERSIANN-CDR (0.31) product is the most efficient among other precipitation products. Lower values of KGE score are found over the northern, northeast, and Western Ghats of India for all the precipitations products. The lower gauge density region is also associated with the lower KGE scores of the multi-satellite precipitation products. Microwave imaging does not give good resolution in cold-freeze areas, due to the high backscatter from the snow. However, ground-based measurement acquires a seasonal variability in the precipitation in these parts efficiently.

The bias values show significant negligence of the precipitation over the western coast and northern region of India. ERA-5 indicates a significant underestimation of precipitation in the northeast region with respect to the IMD product due to the complex precipitation system in these parts. A considerable bias is also observed near the western coast along the windward side. However, a lower bias on the leeward side is demonstrated by all four products, which indicates an overestimation of the precipitation observation. To represent the variability in monthly precipitation across India, a spatial distribution of the coefficient of variation (CV, percent) by all five datasets is shown in Figure 6. The highest variability is shown in the Northwest part of India by all five datasets. However, a difference in the magnitudes of variability ratio is visible among all five datasets. Except for the IMD-gauge-based precipitation product, the other four show very low variability in the Ladakh-Siachin region, while the temperature and moisture govern the variation in these parts. The northwest region of India shows high variability in terms of monthly precipitation, largely governed by the annual monsoon pattern. A qualitative comparison can be observed at spatial levels in India (Figures 5 and 6). All four products can capture significant amounts of precipitation in the country though, and CHIRPS shows the highest variability among others. Over the northern region, NASA POWER tends to achieve the highest variability concerning the IMD-gauge-based observation.

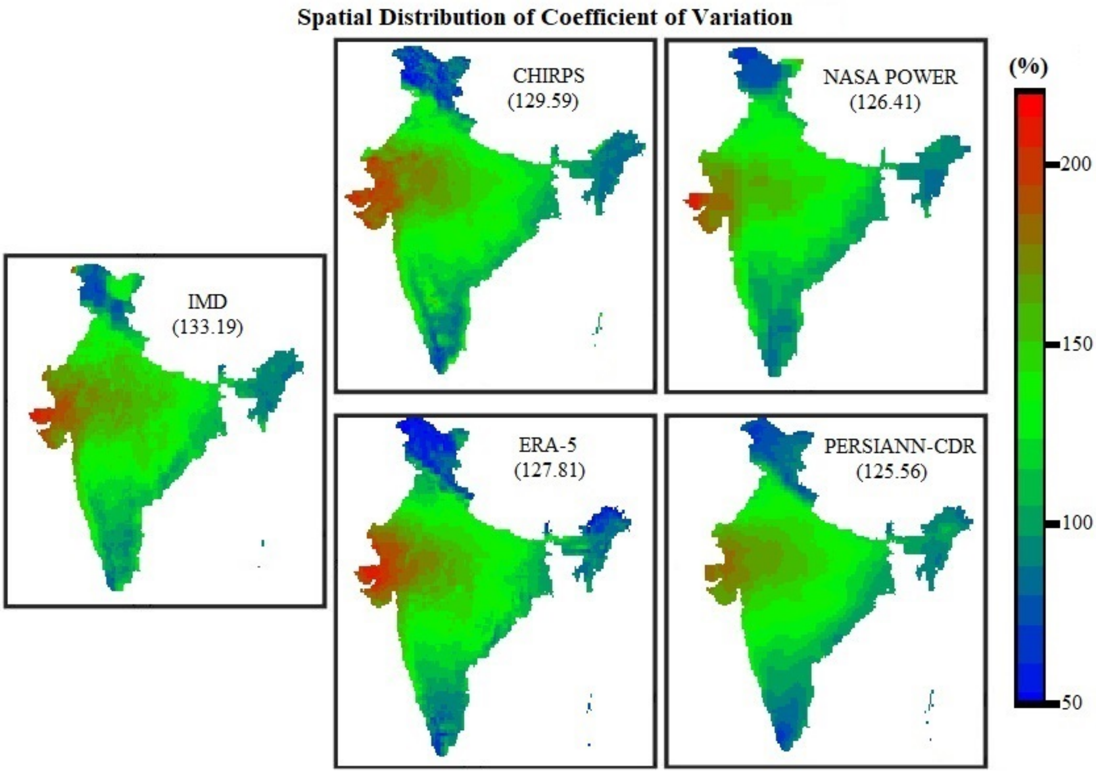

Figure 6. The spatial distribution of coefficient of variation (CV, percent) in yearly precipitation across India at pixel level from IMD, NASA POWER, CHIRPS, ERA-5, and PERSIANN-CDR during the time period 1990–2021. All-India mean values of CV (percent) are also provided in the figure.

3.3. Performance of Precipitation Products over Sub Regions at Pixel Level

The mean values of performance parameters, viz., correlation coefficient, RMSE, systematic error (percent), bias, and variability ratio, is obtained for the precipitation products of CHIRPS, NASA POWER, ERA-5, and PERSIAN-CDR concerning IMD-gauge-based precipitation data over four sub regions of India, namely, Central India, Northeast India, Northwest India, and South Peninsula computed at the pixel level on yearly time scales. The mean estimated values at the pixel level over Central India, Northeast India, Northwest India, and South Peninsula of these performance parameters are shown in Tables 3–6, respectively. Over the central India region, the mean values of the correlation coefficient are obtained at the pixel level as 0.62, 0.593, 0.59, and 0.50 for PERSIANN-CDR, ERA-5, NASA POWER, and CHIRPS, respectively. PERSIANN-CDR demonstrates the highest correlation with the IMD-gauge-based precipitation product (0.62) and CHIRPS shows the lowest (0.50) correlation. The values of RMSE (mm/day) are 0.94, 0.86, 0.79, and 0.83 for PERSIANN-CDR, ERA-5, NASA POWER, and CHIRPS, respectively. The lowest RMSE is found to be 0.79 for NASA POWER, while the highest value is found to be 0.94 for PERSIANN-CDR. The mean systematic error is obtained for CHIRPS, NASA POWER, ERA-5, and PERSIANN-CDR as 4.244, 3.754, 4.824, and 4.404 percent, respectively, and the mean bias is found to be 0.0994 mm/day for CHIRPS, 0.033 mm/day for NASA POWER, −0.08 mm/day for ERA-5, and −0.11 mm/day for PERSIANN-CDR. The lowest values of systematic error and bias are observed in the case of NASA POWER, and the highest value of bias is found for PERSIANN-CDR. The variability ratio is mathematically estimated as 0.98 for CHIRPS, 0.94 for NASA POWER, 1.00 for ERA-5, and 0.95 for PERSIANN-CDR. Furthermore, the mean values of modified KGE score are numerically estimated for CHIRPS, NASA POWER, ERA-5, and PERSIANN-CDR as 0.27, 0.40, 0.39, and 0.42, respectively. Negative bias is observed for ERA-5 and PERSIANN-CDR, while CHIRPS and PERSIANN-CDR receive positive bias. Negative bias suggests the underperformance of the product over the target area, while positive bias represents the over performance of the product. The lowest bias is found for NASA POWER, while the highest value of bias is found for PERSIANN-CDR. For example, the performance of NASA POWER and PERSIANN-CDR is found to be better than the other two precipitation products by the evaluation based on the performance indices. However, CHIRPS and ERA-5 have larger variability ratios, i.e., 0.98 and 1.00, respectively, which exhibits the higher variability of the product over the central India region than other precipitation products. The RMSE, systematic error, and bias suggest the better performance of NASA POWER, while the other two performance indices of correlation coefficients and KGE score suggest the better performance of PERSIANN-CDR over central India. Moreover, KGE ratio suggests that the PERSIANN-CDR dataset performs best in central India. The variability ratio is found to be approximately the same for NASA POWER and PERSIANN-CDR precipitation products. Overall, NASA POWER and PERSIANN-CDR are better multi-satellite products to be used for the assessment of precipitation in central India.

Table 3. Computed mean values of the performance indices over central India region at pixel level for multi-satellite precipitation product against IMD gridded datasets on yearly time scale.

CENTRAL INDIA				
	CHIRPS	**NASA-POWER**	**ERA-5**	**PERSIANN-CDR**
Correlation coefficient	0.50	0.59	0.59	0.62
RMSE (mm day^{-1})	0.83	0.79	0.86	0.94
Systematic Error (%)	4.244	3.754	4.824	4.404
Bias	0.0994	0.033	−0.08	−0.11
Variability Ratio	0.98	0.94	1.00	0.95
KGE	0.27	0.40	0.39	0.42

Table 4. Computed mean values of the performance indices over Northeast India region at pixel level for multi-satellite precipitation product against IMD gridded datasets in yearly time scale.

NORTHEAST INDIA				
	CHIRPS	**NASA-POWER**	**ERA-5**	**PERSIANN-CDR**
Correlation coefficient	0.35	0.30	0.41	0.44
RMSE (mm day^{-1})	1.85	1.86	2.61	2.06
Systematic Error (%)	11.04	8.76	12.75	11.92
Bias	0.07	0.83	−1.43	0.08
Variability Ratio	0.96	0.968	0.93	0.982
KGE	0.054	−0.01	0.049	0.15

Table 5. Computed mean values of the performance indices over northwest India region at pixel level for multi-satellite precipitation product against IMD gridded datasets on yearly time scale.

NORTHWEST INDIA				
	CHIRPS	**NASA-POWER**	**ERA-5**	**PERSIANN-CDR**
Correlation coefficient	0.40	0.38	0.50	0.50
RMSE (mm day^{-1})	0.95	0.94	0.917	0.87
Systematic Error (%)	1.94	1.89	2.23	2.02
Bias	0.18	0.42	−0.15	0.05
Variability Ratio	0.94	0.94	0.90	0.93
KGE	0.09	0.07	0.22	0.24

Table 6. Computed mean values of the performance indices over South Peninsula region at pixel level for multi-satellite precipitation product against IMD gridded datasets on yearly time scale.

SOUTH PENINSULA				
	CHIRPS	**NASA-POWER**	**ERA-5**	**PERSIANN-CDR**
Correlation coefficient	0.46	0.53	0.54	0.53
RMSE (mm day^{-1})	0.99	0.95	1.01	1.22
Systematic Error (%)	4.32	2.74	5.40	5.05
Bias	−0.08	−0.001	−0.15	−0.25
Variability Ratio	0.98	0.94	0.96	0.92
KGE	0.21	0.31	0.31	0.25

The mean values of performance parameters over the northeast India region computed at the pixel level on yearly time scales for the precipitation products of CHIRPS, NASA POWER, ERA-5, and PERSIANN-CDR are given in Table 4. Higher values of mean correlation coefficients and KGE score are found for PERSIANN-CDR. Lower values of RMSE, systematic error, bias, and variability ratio are found for CHIRPS, NASA-POWER, CHIRPS, and ERA-5, respectively. The observation based on the values of performance indices, namely, RMSE, systematic error, bias, and variability ratio, suggests that the CHIRPS precipitation dataset has better performance than the other three precipitation dataset over northeast India. The two performance indices (RMSE and bias) out of four (RMSE, systematic error, bias, and variability ratio) support the CHIRPS precipitation dataset. PERSIANN-CDR shows better performance according to the correlation coefficients and KGE score. However, the CHIRPS precipitation dataset shows the better performance according to the other two performance indices (RMSE and bias). For example, both precipitation datasets (CHIRPS, and PERSIANN-CDR) show the better performance over northeast India.

The mean values of the correlation coefficient between various precipitation products (PERSIANN-CDR, ERA-5, NASA POWER, and CHIRPS) and IMD gridded precipitation are found to be 0.50, 0.50, 0.38, and 0.40 over Northwest India computed at the pixel level on yearly time scales for the long term of 30+ years (1990–2021), given in Table 5. The highest value of correlation coefficients is found for the PERSIANN-CDR and ERA-5 datasets. The lowest values of RMSE, systematic error, bias, and variability ratio are 0.87 mm/day, 1.89 percent, 0.05, and 0.90 for the PERSIANN-CDR, NASA POWER, PERSIANN-CDR, and ERA-5 datasets, respectively. The performance of the PERSIANN-CDR precipitation dataset is significantly better from the evaluation of the values of four performance indices (RMSE, systematic error, bias, and variability ratio) because two performance indices (RMSE and bias) show lower values for the PERSIANN-CDR dataset than the other precipitation datasets. A higher value of KGE score (0.24) is also found for the PERSIANN-CDR precipitation dataset. The correlation coefficient and KGE score show the better performance of PERSIANN-CDR compared to the other precipitation datasets. From the observations made, it can be concluded that the PERSIANN-CDR precipitation dataset performs better compared to other precipitation dataset over Northwest India.

The mean values of performance parameters of the precipitation products (CHIRPS, NASA POWER, ERA-5, and PERSIANN-CDR) with respect to the IMD rain gauge gridded dataset over the South Peninsula region computed at the pixel level on yearly time scales for the 30+ years (1990–2021) are reported in Table 6. The correlation of the multi-satellite precipitation product of CHIRPS, NASA POWER, ERA-5, and PERSIANN-CDR with IMD-gauge-based precipitation products is found to be 0.46, 0.53, 0.54, and 0.53, respectively. The RMSE values are obtained for CHIRPS, NASA POWER, ERA-5, and PERSIANN-CDR as 0.99 mm/day, 0.95 mm/day, 1.01 mm/day, and 1.22 mm/day, respectively. The systematic errors are found for CHIRPS (4.32 percent), NASA POWER (2.74 percent), ERA-5

(5.40 percent), and PERSIANN-CDR (5.05 percent). The values of bias are obtained as −0.08, −0.001, −0.15, and −0.25 for the precipitation products of CHIRPS, NASA POWER, ERA-5, and PERSIANN-CDR against the IMD dataset, respectively. Furthermore, the values of variability ratio are found for CHIRPS (0.98), NASA POWER (0.94), ERA-5 (0.96), and PERSIANN-CDR (0.92). The KGE score is determined for CHIRPS (0.21), NASA POWER (0.31), ERA-5 (0.31), and PERSIANN-CDR (0.25). The performance of the NASA-POWER precipitation product is found to be better than those of the other precipitation products (CHIRPS, ERA-5, and PERSIANN-CDR) over the South Peninsula of India.

The yearly mean value of rainfall is found below 7 mm/day for all the regions for every year (see Figure 3b). A slightly higher value of yearly mean rainfall (~7.6 mm/day) is found over the northeast region (maximum number of rainfall events occurs in this region) for very few years. The optimum threshold value of rainfall (7 mm/day) is considered to analyze the performance of multi-satellite precipitation data products because this threshold has a tendency to cover all the datasets for the years having limited (below 7 mm/day) and higher (above 7 mm/day) extreme rainfall events. Table 7 represents the mean values of the performance indices over various regions (India, Central India, Northwest, Northeast, and South Peninsula) computed at the pixel level on a yearly time scale for two different states (which is the rainfall recorded below 7 mm/day and above 7 mm/day). In the case of the yearly mean rainfall recorded between 0 and 7 mm/day, the higher values of mean correlation coefficients over India and its sub regions are found to be 0.53, 0.64, 0.51, 0.48, and 0.56 for ERA-5 (better for India region) and PERSIANN-CDR (better for Central India, Northwest, Northeast, and South Peninsula regions) computed at the pixel level on yearly time scales. The minimum values of mean RMSE over the India, Central India, and South Peninsula regions computed at the pixel level on yearly time scales for the NASA POWER dataset are found to be 0.93 mm/day, 0.72 mm/day, and 0.84 mm/day, respectively, while lower values of mean RMSE over the Northwest and Northeast for the PERSIANN-CDR and CHIRPS datasets are found to be 0.87 mm/day and 1.47 mm/day, respectively. The mean values of the variability ratio are found to be approximately the same (between 0.93 and 1.01) over India and its sub regions for all the precipitation datasets. The mean higher values of KGE score over India, Central India, Northwest, and Northeast regions computed at the pixel level on yearly time scales are found to be 0.32, 0.44, 0.25, and 0.21 for the PERSIANN-CDR datasets, while the mean of the higher value is found to be 0.33 over the South Peninsula region for NASA POWER and ERA-5 datasets. The comparison of the performance indices computed at the pixel level suggests that the PERSIANN-CDR datasets perform better over sub regions for the yearly mean rainfall between 0 and 7 mm/day. However, no conclusive evidence is found to suggest the better-performing datasets over the India region for yearly mean rainfall between 0 and 7 mm/day.

The maximum mean values of the correlation coefficient over India, Central India, Northeast, and South Peninsula computed at the pixel level are found to be 0.44, 0.67, 0.40, and 0.43 with NASA POWER, ERA-5, NASA POWER, and ERA-5 for yearly mean rainfall above 7 mm/day, respectively. The minimum mean value of RMSE is found to be 3.05 mm/day and 2.58 mm/day over the Central India and South Peninsula regions computed at the pixel level on yearly time scales for the ERA-5 dataset, while the minimum value of RMSE is found to be 3.69 and 0.94 over the India and Northeast regions for CHIRPS and PERSIANN-CDR datasets, respectively. The variability ratio is found at the same values for various datasets over all the regions. The higher mean values of KGE score over India, Central India, Northeast, and South Peninsula regions computed at the pixel level on yearly time scales are found to be 0.25, 0.46, 0.27, and 0.41 for PERSIANN-CDR, ERA-5, CHIRPS and PERSIANN-CDR, respectively. The ERA-5 dataset performs better over the Central India and South Peninsula regions at the pixel level on yearly time scales for yearly mean rainfall above 7 mm/day. However, no conclusive evidence is found to suggest the better-performing datasets over India and the Northeast region for yearly mean rainfall above 7 mm/day.

Table 7. Computed mean values of the performance indices over various regions at pixel level for multi-satellite precipitation product against IMD gridded datasets on yearly time scales for two levels of rainfall. Dashes in cells represent no data value.

Region Name ↓	Indices →	R (Mean)		RMSE (Mean)		Variability Ratio (Mean)		KGE (Mean)	
	Data Products ↓	**Rainfall (0–7) mm/day**	**Rainfall (7–above) mm/day**	**Rainfall (0–7) mm/day**	**Rainfall (7–above) mm/day**	**Rainfall (0–7) mm/day**	**Rainfall (7–above) mm/day**	**Rainfall (0–7) mm/day**	**Rainfall (7–above) mm/day**
India	CHIRPS	0.44	0.28	0.96	3.69	0.97	0.98	0.18	−0.07
	NASA POWER	0.47	0.44	0.93	3.88	0.95	0.97	0.22	0.13
	ERA 5	0.53	0.42	1.08	3.97	0.96	0.90	0.28	0.08
	PERSIANN CDR	0.21	0.29	0.99	4.92	0.95	0.91	0.32	−0.25
Central India	CHIRPS	0.50	0.46	0.77	3.64	0.99	0.96	0.28	0.16
	NASA POWER	0.60	0.63	0.72	3.93	0.95	0.95	0.41	0.35
	ERA 5	0.59	0.67	0.81	3.05	1.01	0.97	0.40	0.46
	PERSIANN CDR	0.64	0.26	0.82	5.42	0.96	0.88	0.44	−0.19
North-West	CHIRPS	0.40	-	0.95	-	0.95	-	0.10	-
	NASA POWER	0.38	-	0.92	-	0.95	-	0.08	-
	ERA 5	0.50	-	0.92	-	0.90	-	0.23	-
	PERSIANN CDR	0.51	-	0.87	-	0.93	-	0.25	-
North-East	CHIRPS	0.39	0.14	1.47	4.28	0.97	0.98	0.10	−0.27
	NASA POWER	0.29	0.40	1.49	4.40	0.97	0.99	−0.02	0.06
	ERA 5	0.44	0.32	2.24	5.04	0.99	0.86	0.07	−0.10
	PERSIANN CDR	0.48	0.22	1.63	0.94	0.98	0.98	0.21	−0.19
South Peninsula	CHIRPS	0.47	0.41	0.90	2.54	0.99	0.99	0.22	0.14
	NASA POWER	0.54	0.39	0.84	2.82	0.94	0.96	0.33	0.10
	ERA 5	0.55	0.43	0.92	2.58	0.97	0.91	0.33	0.17
	PERSIANN CDR	0.56	0.06	1.02	4.65	0.93	0.81	0.30	−0.41

Figure 7 presents comparative representations of empirical cumulative distribution functions among the monthly mean of all five precipitation products across India, Central India, the West coast, and Northeast for the period of 1990–2021. It is observed that the ground-based observation coincides with the satellite-based products in central India better than in the Northeast. The sparse gauge density in the northeast might be the possible reason for this difference. Nevertheless, all products perform quite well while representing the whole country. PERSIANN-CDR and ERA-5 give the best agreement with the IMD-gauge-based precipitation dataset. Moreover, NASA POWER seems to overestimate the moderate precipitation despite the other products and require further improvement to make it analogous to other multi-satellite precipitation datasets. In addition, the NASA power precipitation product CDF seems to coincide with the IMD over the South Peninsula of India.

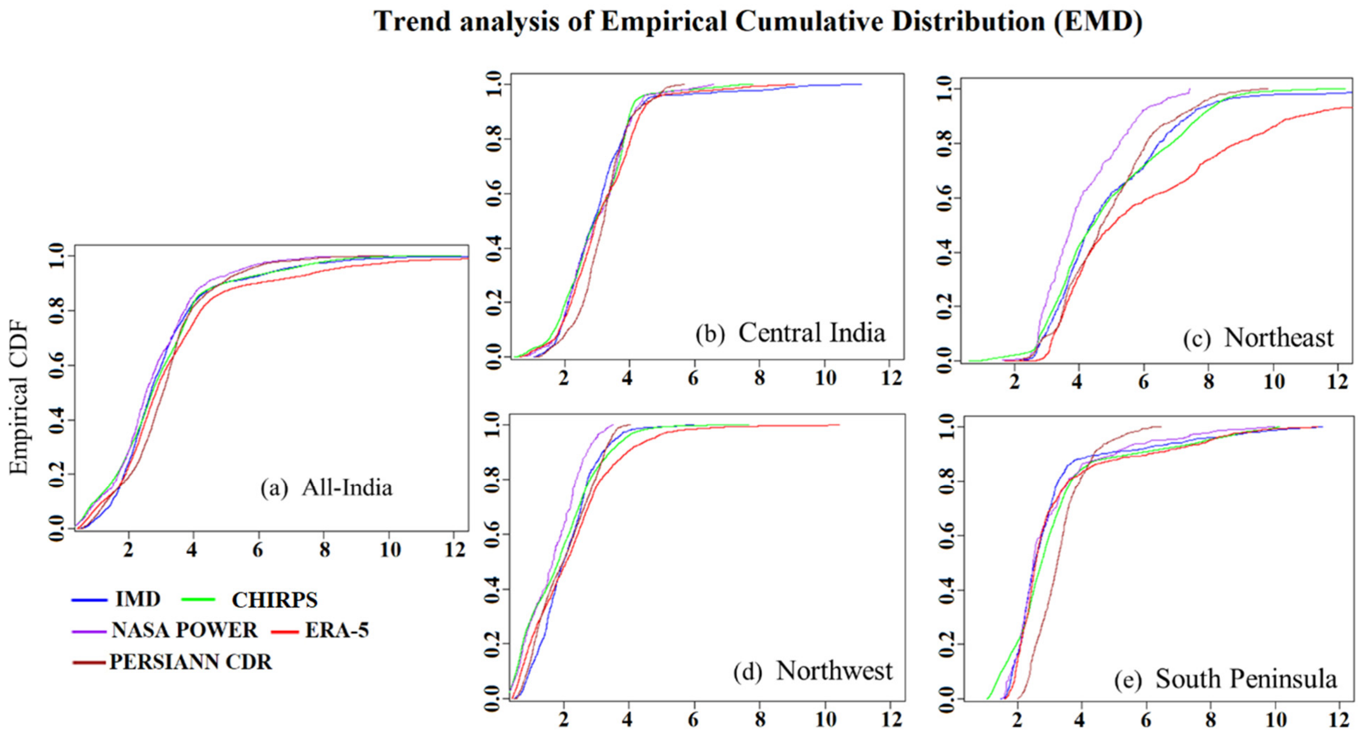

Figure 7. Trend analysis of the empirical cumulative distribution (EMD) functions of monthly precipitation derived from the IMD, NASA POWER, CHIRPS, ERA-5, and PERSIAN-CDR products across (**a**) all India, (**b**) Central India, (**c**) Northeast, (**d**) West Coast, and (**e**) South Peninsula for the period of 1990–2021.

Another method based on the Taylor's diagram is used to identify the comparative uncertainty for the comparative study of various precipitation products over India and its sub regions [42]. Taylor's diagrams are produced for the monthly average precipitation from IMD, CHIRPS, NASA POWER, and ERA-5 over Central India, the Northeast, the Northwest, and the South Peninsula of India for 1990 to 2021. Figure 8 shows the Taylor's plot for the monthly precipitation derived from CHIRPS, NASA POWER, ERA-5, and PERSIANN-CDR corresponding to the rain-gauge-based IMD product over India for the time period of 1990–2021. A similar precipitation modeling group shows similar performance as they lie close to each other on Taylor's diagram. The higher all-India mean precipitation in the monsoon season is well captured by each product. However, considerable efficiency and performance are found in ERA-5 and PERSIANN-CDR. These products have the potential ability to model precipitation trends in India in the future as well. Taylor's diagram clearly shows that CHIRPS, ERA-5, and PERSIANN-CDR are the good multi-satellite products among all test products except NASA POWER. It has also been noted that all the products need improvement over the northeastern region. Furthermore, CHIRPS and PERSIANN-CDR perform almost indistinguishably in northeast India. NASA POWER, on the other hand, performs inadequately compared with the other models. Taylor's graphic displayed for sub regions of India is displayed in Figure 9a–d. The NASA POWER precipitation product also shows the best match with the IMD precipitation datasets in the South Peninsula sub regions of Taylor's diagram.

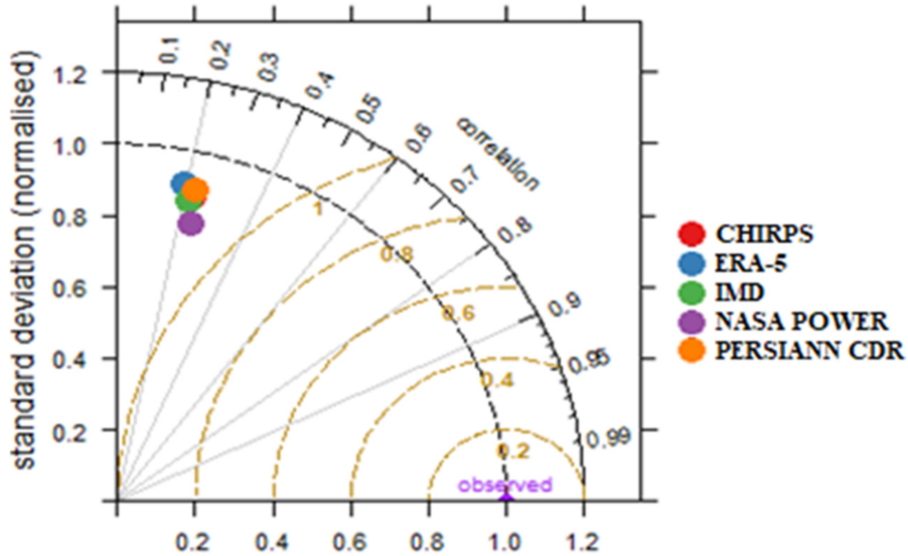

Figure 8. Taylor's diagram for the monthly all-India precipitation derived from CHIRPS, NASA POWER, ERA-5, and PERSIANN-CDR corresponding to rain-gauge-based IMD product for the period of 1990–2021.

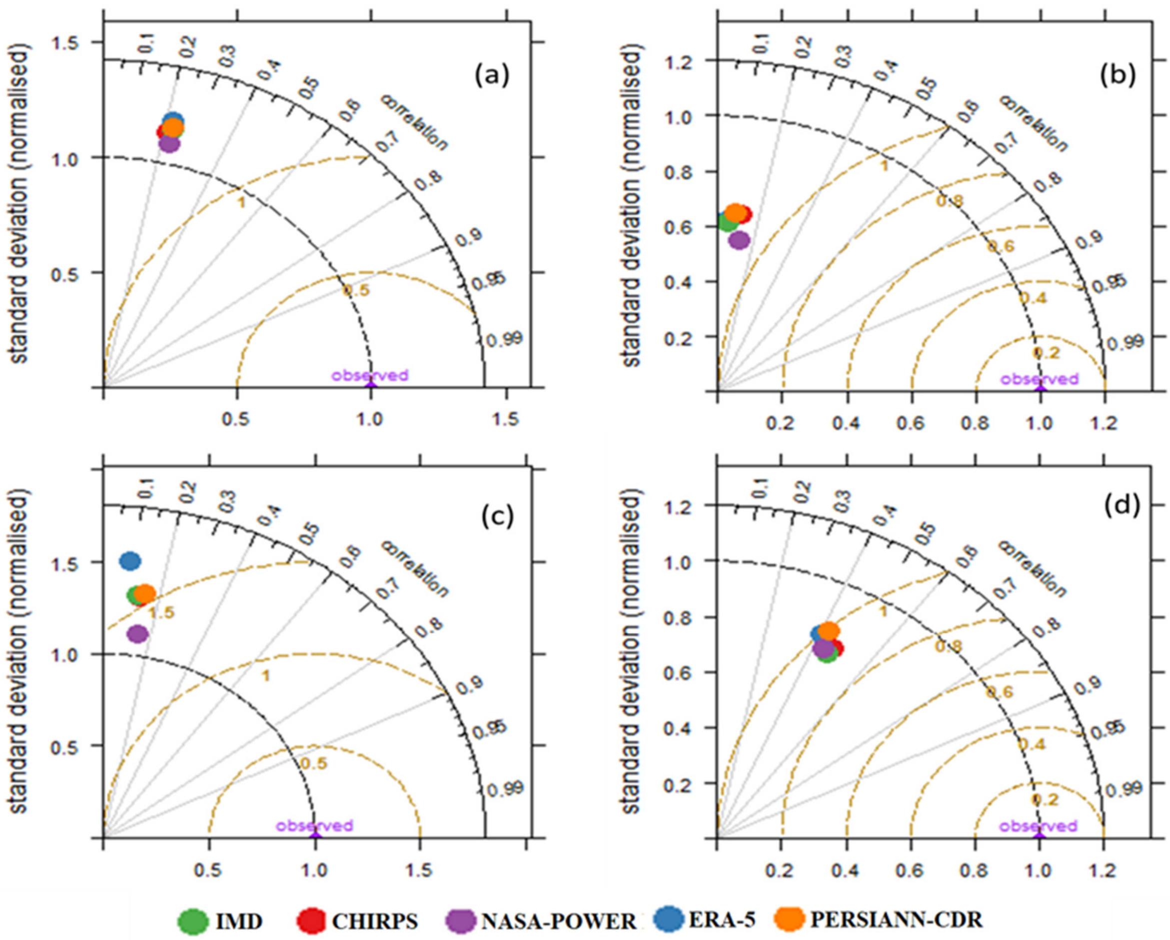

Figure 9. Taylor's diagrams comparing performances of monthly average precipitation estimation obtained from IMD, CHIRPS, NASA POWER, ERA-5, and PERSIANN-CDR in (**a**) Central India, (**b**) Northwest, (**c**) Northeast, and (**d**) South Peninsula for the period of 1990–2021.

Overall, PERSIANN-CDR performs better in Central India, Northeast India, and Northwest India, whereas the NASA-POWER precipitation product performs better in Central India and South Peninsular India. The other two precipitation products (CHIRPS, and ERA-5) show intermediate performance over various sub regions of India.

4. Conclusions

In the present investigation an extensive evaluation of the latest version of multi-satellite-based precipitation products, i.e., CHIRPS version 2.0, NASA POWER, ERA-5, and PERSIANN-CDR, was carried out using the rain gauge interpolated precipitation product of IMD across India at regional, sub regional, and pixel levels for monthly and yearly time scales. The study was conducted across India and its subdivisions such as Central India, Northwest, Northeast, and South Peninsula for the time duration of 30+ years from 1990 to 2021.

The results obtained from the various analyses, i.e., regression, KGE score, RMSE, and bias score, signify the high usability and better performance of satellite-derived precipitation datasets against gauged IMD precipitation datasets. All the precipitation products perform better on monthly than yearly time scales at the regional scale. The results indicate that PERSIANN-CDR and ERA-5 products perform significantly well for the extensive study of precipitation in the context of the Indian subcontinent at the pixel level. The IMD-retrieved data show a mean precipitation in India of 3.05 mm/day, whereas CHIRPS and NASA POWER underestimate and ERA-5 and PERSIANN-CDR overestimate the mean values concerning the IMD dataset. In addition, PERSIANN-CDR performs better in Central India, Northeast India, and Northwest India, whereas the NASA-POWER precipitation product performs better in Central India and South Peninsula India. Two other precipitation products (CHIRPS and ERA-5) show intermediate performance over various sub regions of India. PERSIANN-CDR performs better in Central India, Northeast India, Northwest India, and South Peninsula when the yearly mean rainfall ranges between 0 and 7 mm/day, while ERA-5 performs better in Central India and the South Peninsula region for yearly mean rainfall above 0–7 mm/day.

The satellite-derived precipitation products are also able to detect the variability in precipitation amount in the Western Ghats during the monsoon months. The hydrological management and climatological applications can be fulfilled using only satellite-based data due to its high spatial applicability on terrain and the ocean. However, these products need to be calibrated regularly to the gauge-based data to improve the future applications and predictions of upcoming hydro-disasters. The uncertainty between the products is compared using the Taylor's diagram and the relative errors are found to be quite indistinguishable for all the precipitation products over all the regions of India. A noticeable difference in the uncertainty is depicted across Northeast India, where the performance of ERA-5 and PERSIANN-CDR is found to be most acceptable for future reference. Although it has been noticed that Northeastern India lacks several gauge-based observational stations, gauge-based observations triumph over satellite-based precipitation products because of the influence of the complex topography and frequent dense cloud formation in this region. Nevertheless, PERSIANN-CDR emerges as the best precipitation product for the assessment of precipitation on the Indian subcontinent. Hence, a good knowledge of long-term spatiotemporal precipitation datasets can improve the understanding of the variability in rainfall over the region, which allows for monitoring the water cycle and upcoming hydro-disasters associated with climate change.

Author Contributions: Conceptualization, D.K.G., G.P.P. and J.N.T.; methodology, D.K.G., J.N.T. and A.K.S.; software, D.K.G. and N.A.; validation, N.A., D.K.G., A.K.K., G.P.P. and J.N.T.; formal analysis, D.K.G., A.K.K. and N.A.; investigation, D.K.G., N.A. and J.N.T.; resources, D.K.G., A.K.S., J.N.T. and G.P.P.; data curation, D.K.G. and N.A.; writing—original draft preparation, D.K.G., A.K.K. and N.A.; writing—review and editing, N.A., D.K.G., G.P.P. and J.N.T.; visualization, D.K.G. and A.K.S.; supervision, J.N.T. and A.K.S.; project administration, J.N.T. and A.K.S.; funding acquisition. All authors have read and agreed to the published version of the manuscript.

Funding: This research received no external funding.

Data Availability Statement: Not applicable.

Acknowledgments: We acknowledge all the data provider agencies given in this manuscript. We also have acknowledged the DS Kothari post-doctoral fellowship provided by UGC India (No. F.4-2/2006 (BSR)/ES/20-21/0011).

Conflicts of Interest: The authors declare no conflict of interest.

References

1. Kidd, C.; Becker, A.; Huffman, G.J.; Muller, C.L.; Joe, P.; Skofronick-Jackson, G.; Kirschbaum, D.B. So, how much of the Earth's surface is covered by rain gauges? *Bull. Am. Meteorol. Soc.* **2017**, *98*, 69–78. [CrossRef]
2. Loo, Y.Y.; Billa, L.; Singh, A. Effect of climate change on seasonal monsoon in Asia and its impact on the variability of monsoon rainfall in Southeast Asia. *Geosci. Front.* **2015**, *6*, 817–823. [CrossRef]
3. Misra, V.; DiNapoli, S. The variability of the Southeast Asian summer monsoon. *Int. J. Climatol.* **2014**, *34*, 893–901. [CrossRef]
4. Dikshit, K.R.; Dikshit, J.K. *North-East India: Land, People and Economy*; Springer: Berlin/Heidelberg, Germany, 2014.
5. Chakraborty, A.; Nanjundiah, R.; Srinivasan, J. Role of Asian and African orography in Indian summer monsoon. *Geophys. Res. Lett.* **2002**, *29*, 50-1–50-4. [CrossRef]
6. Menon, A.; Levermann, A.; Schewe, J.; Lehmann, J.; Frieler, K. Consistent increase in Indian monsoon rainfall and its variability across CMIP-5 models. *Earth Syst. Dyn.* **2013**, *4*, 287–300. [CrossRef]
7. Sunilkumar, K.; Narayana Rao, T.; Saikranthi, K.; Purnachandra Rao, M. Comprehensive evaluation of multisatellite precipitation estimates over India using gridded rainfall data. *J. Geophys. Res. Atmos.* **2015**, *120*, 8987–9005. [CrossRef]
8. Chauhan, A.S.; Singh, S.; Maurya, R.K.S.; Kisi, O.; Rani, A.; Danodia, A. Spatio-temporal analysis of rainfall dynamics of 120 years (1901–2020) using innovative trend methodology: A case study of Haryana, India. *Sustainability* **2022**, *14*, 4888. [CrossRef]
9. Bushair, M.; Prakash, S.; Patel, S.; Gairola, R. Assessment of Kalpana-1 rainfall product over Indian meteorological sub-divisions during the summer monsoon season. *J. Indian Soc. Remote Sens.* **2016**, *44*, 67–76. [CrossRef]
10. Singh, A.K.; Singh, V.; Singh, K.; Tripathi, J.; Kumar, A.; Sateesh, M.; Peshin, S. Validation of INSAT-3D derived rainfall estimates (HE & IMSRA), GPM (IMERG) and GLDAS 2.1 model rainfall product with IMD gridded rainfall & NMSG data over IMD's meteorological sub-divisions during monsoon. *Mausam* **2018**, *69*, 177–192.
11. Durai, V.; Bhowmik, S.R.; Mukhopadhyay, B. Evaluation of Indian summer monsoon rainfall features using TRMM and KALPANA-1 satellite derived precipitation and rain gauge observation. *Mausam* **2010**, *61*, 317–336. [CrossRef]
12. Mahesh, C.; Prakash, S.; Gairola, R.; Shah, S.; Pal, P. Meteorological Sub-divisional Scale Rainfall Monitoring Using K alpana-1 VHRR Measurements. *Geogr. Res.* **2014**, *52*, 328–336. [CrossRef]
13. Prakash, S.; Gairola, R.M. Large-scale precipitation estimation using Kalpana-1 IR measurements and its validation using GPCP and GPCC data. *Theor. Appl. Climatol.* **2011**, *106*, 283–293. [CrossRef]
14. Huffman, G.J.; Adler, R.F.; Arkin, P.; Chang, A.; Ferraro, R.; Gruber, A.; Janowiak, J.; McNab, A.; Rudolf, B.; Schneider, U. The global precipitation climatology project (GPCP) combined precipitation dataset. *Bull. Am. Meteorol. Soc.* **1997**, *78*, 5–20. [CrossRef]
15. Huffman, G.J.; Bolvin, D.T.; Nelkin, E.J.; Wolff, D.B.; Adler, R.F.; Gu, G.; Hong, Y.; Bowman, K.P.; Stocker, E.F. The TRMM multisatellite precipitation analysis (TMPA): Quasi-global, multiyear, combined-sensor precipitation estimates at fine scales. *J. Hydrometeorol.* **2007**, *8*, 38–55. [CrossRef]
16. Setti, S.; Maheswaran, R.; Sridhar, V.; Barik, K.K.; Merz, B.; Agarwal, A. Inter-comparison of gauge-based gridded data, reanalysis and satellite precipitation product with an emphasis on hydrological modeling. *Atmosphere* **2020**, *11*, 1252. [CrossRef]
17. Kling, H.; Fuchs, M.; Paulin, M. Runoff conditions in the upper Danube basin under an ensemble of climate change scenarios. *J. Hydrol.* **2012**, *424*, 264–277. [CrossRef]
18. Yong, B.; Liu, D.; Gourley, J.J.; Tian, Y.; Huffman, G.J.; Ren, L.; Hong, Y. Global view of real-time TRMM multisatellite precipitation analysis: Implications for its successor global precipitation measurement mission. *Bull. Am. Meteorol. Soc.* **2015**, *96*, 283–296. [CrossRef]
19. Prakash, S.; Mitra, A.K.; AghaKouchak, A.; Liu, Z.; Norouzi, H.; Pai, D. A preliminary assessment of GPM-based multi-satellite precipitation estimates over a monsoon dominated region. *J. Hydrol.* **2018**, *556*, 865–876. [CrossRef]
20. Prakash, S.; Mitra, A.K.; Gairola, R.M.; Norouzi, H.; Pai, D.S. Status of high-resolution multisatellite precipitation products across India. In *Remote Sensing of Aerosols, Clouds, and Precipitation*; Elsevier: Amsterdam, The Netherlands, 2018; pp. 301–314.
21. Prakash, S.; Mitra, A.K.; Pai, D.; AghaKouchak, A. From TRMM to GPM: How well can heavy rainfall be detected from space? *Adv. Water Resour.* **2016**, *88*, 1–7. [CrossRef]
22. Hoffmann, L.; Günther, G.; Li, D.; Stein, O.; Wu, X.; Griessbach, S.; Heng, Y.; Konopka, P.; Müller, R.; Vogel, B. From ERA-Interim to ERA5: The considerable impact of ECMWF's next-generation reanalysis on Lagrangian transport simulations. *Atmos. Chem. Phys.* **2019**, *19*, 3097–3124. [CrossRef]
23. Funk, C.; Peterson, P.; Landsfeld, M.; Pedreros, D.; Verdin, J.; Shukla, S.; Husak, G.; Rowland, J.; Harrison, L.; Hoell, A. The climate hazards infrared precipitation with stations—A new environmental record for monitoring extremes. *Sci. Data* **2015**, *2*, 150066. [CrossRef] [PubMed]

24. Wiwoho, B.S.; Astuti, I.S.; Alfarizi, I.A.G.; Sucahyo, H.R. Validation of three daily satellite rainfall products in a humid tropic watershed, Brantas, Indonesia: Implications to land characteristics and hydrological modelling. *Hydrology* **2021**, *8*, 154. [CrossRef]
25. Saicharan, V.; Rangaswamy, S.H. A Comparison and Ranking Study of Monthly Average Rainfall Datasets with IMD Gridded Data in India. *Sustainability* **2023**, *15*, 5758. [CrossRef]
26. Dubey, R.K.; Dubey, P.K.; Chaurasia, R.; Rao, C.S.; Abhilash, P.C. Impact of integrated agronomic practices on soil fertility and respiration on the Indo-Gangetic Plain of North India. *Agronomy* **2021**, *11*, 402. [CrossRef]
27. Dubey, S.; Gupta, H.; Goyal, M.K.; Joshi, N. Evaluation of precipitation datasets available on Google earth engine over India. *Int. J. Climatol.* **2021**, *41*, 4844–4863. [CrossRef]
28. Gorelick, N.; Hancher, M.; Dixon, M.; Ilyushchenko, S.; Thau, D.; Moore, R. Google Earth Engine: Planetary-scale geospatial analysis for everyone. *Remote Sens. Environ.* **2017**, *202*, 18–27. [CrossRef]
29. Singh, P.; Nautiyal, O.; Joshi, M.; Kumar, A.; Ahamad, T.; Singh, K. Assessment of physicochemical and radon-attributable radiological parameters of drinking water samples of Pithoragarh district, Uttarakhand. *J. Radioanal. Nucl. Chem.* **2021**, *330*, 1559–1570. [CrossRef]
30. Rao, K.K.; Kulkarni, A.; Patwardhan, S.; Kumar, B.V.; Kumar, T. Future changes in precipitation extremes during northeast monsoon over south peninsular India. *Theor. Appl. Climatol.* **2020**, *142*, 205–217. [CrossRef]
31. Singh, K.P.; Malik, A.; Singh, V.K.; Mohan, D.; Sinha, S. Chemometric analysis of groundwater quality data of alluvial aquifer of Gangetic plain, North India. *Anal. Chim. Acta* **2005**, *550*, 82–91. [CrossRef]
32. Singh, J.; Roy, P.; Murthy, M.; Jha, C.S. Application of landscape ecology and remote sensing for assessment, monitoring and conservation of biodiversity. *J. Indian Soc. Remote Sens.* **2010**, *38*, 365–385. [CrossRef]
33. Nandy, S. Agro-Economic Indicators—A Comparative Study of North-Eastern States of India. *J. Land Rural. Stud.* **2014**, *2*, 75–88. [CrossRef]
34. Widdowson, M. Tertiary palaeosurfaces of the SW Deccan, Western India: Implications for passive margin uplift. *Geol. Soc. Lond. Spec. Publ.* **1997**, *120*, 221–248. [CrossRef]
35. Pai, D.; Rajeevan, M.; Sreejith, O.; Mukhopadhyay, B.; Satbha, N. Development of a new high spatial resolution (0.25×0.25) long period (1901–2010) daily gridded rainfall data set over India and its comparison with existing data sets over the region. *Mausam* **2014**, *65*, 1–18. [CrossRef]
36. Prakash, S.; Mitra, A.K.; Momin, I.M.; Pai, D.; Rajagopal, E.; Basu, S. Comparison of TMPA-3B42 versions 6 and 7 precipitation products with gauge-based data over India for the southwest monsoon period. *J. Hydrometeorol.* **2015**, *16*, 346–362. [CrossRef]
37. Ashouri, H.; Hsu, K.-L.; Sorooshian, S.; Braithwaite, D.K.; Knapp, K.R.; Cecil, L.D.; Nelson, B.R.; Prat, O.P. PERSIANN-CDR: Daily precipitation climate data record from multisatellite observations for hydrological and climate studies. *Bull. Am. Meteorol. Soc.* **2015**, *96*, 69–83. [CrossRef]
38. Gupta, H.V.; Kling, H.; Yilmaz, K.K.; Martinez, G.F. Decomposition of the mean squared error and NSE performance criteria: Implications for improving hydrological modelling. *J. Hydrol.* **2009**, *377*, 80–91. [CrossRef]
39. Knoben, W.J.; Freer, J.E.; Woods, R.A. Inherent benchmark or not? Comparing Nash–Sutcliffe and Kling–Gupta efficiency scores. *Hydrol. Earth Syst. Sci.* **2019**, *23*, 4323–4331. [CrossRef]
40. Rahman, S.; Sengupta, D.; Ravichandran, M. Variability of Indian summer monsoon rainfall in daily data from gauge and satellite. *J. Geophys. Res. Atmos.* **2009**, *114*. [CrossRef]
41. Tiwari, S.; Jha, S.K.; Singh, A. Quantification of node importance in rain gauge network: Influence of temporal resolution and rain gauge density. *Sci. Rep.* **2020**, *10*, 9761. [CrossRef]
42. Taylor, K.E. Summarizing multiple aspects of model performance in a single diagram. *J. Geophys. Res. Atmos.* **2001**, *106*, 7183–7192. [CrossRef]

Disclaimer/Publisher's Note: The statements, opinions and data contained in all publications are solely those of the individual author(s) and contributor(s) and not of MDPI and/or the editor(s). MDPI and/or the editor(s) disclaim responsibility for any injury to people or property resulting from any ideas, methods, instructions or products referred to in the content.